

Protecting group/halogen effect of *N*-glycosylamines on the self assembly of organogelator

Subbiah Nagarajan,^a Pawar Ravinder,^b Venkatesan Subramanian^b and Thangamuthu Mohan Das^{*a}

Received (in Gainesville, FL, USA) 12th August 2009, Accepted 29th September 2009

First published as an Advance Article on the web 5th November 2009

DOI: 10.1039/b9nj00400a

A series of *N*-glycosylamine based organogelators were synthesised from three different 4,6-*O*-protected saccharides. All these compounds were characterized using different spectral techniques. The effect of substituents present in the *N*-glycosylamines on gelation was studied from NMR and computation. Among the eighteen different gelators studied, **3b**, bearing fluorine as a substituent, was observed to gelate at very low concentrations (CGC: 1%). Further, it is revealed that dipole–dipole interactions play an important role in the case of *N*-glycosylamine-based gelators. The presence of π – π stacking and H-bonding, as inferred from the reported X-ray diffraction data, are responsible for the gelation. Various possible modes of interaction are identified from computational studies. The gelation properties of these compounds were studied with regard to their molecular structure by scanning electron microscopy, differential scanning calorimetry, FT-IR and NMR studies.

Introduction

In recent years, low molecular weight organogelators (LMOGs) have played an important role in the field of materials.¹ Some of the sugar-based derivatives possessing strong H-bond-forming segments are prone to form gels even at low concentration.² Molecular self assembly is becoming a popular tool to construct different types of micro- and nano-structured materials.³ LMOGs are known as distinct soft materials and can self-assemble into various types of fibrils, strands, and tapes in organic solvents *via* weak intermolecular interactions.⁴ In an organogel medium, one dimensional (1D) supramolecular fibers are bundled up together and entangled at nodes, so-called “junction points”, to form three-dimensional (3D) network structures, which entrap the solvent molecules. The nanostructured functional molecular assembly thus created is a promising candidate for organic devices with intriguing photo- and electrochemical functions.⁵ In the present case, H-bonding, CH– π , π – π stacking and dipole–dipole interactions seem to play an important role in self assembly. In order to obtain further insight into the structure–function relationship of sugar-based organogelators, we have generated a library of *N*-glycosylamines.

Results and discussion

Synthesis and characterisation of *N*-glycosylamines

4,6-*O*-Butylidene-D-glucopyranose (BGP) **2a**, 4,6-*O*-ethylidene-D-glucopyranose (EGP) **2b** and 4,6-*O*-benzylidene-D-glucopyranose

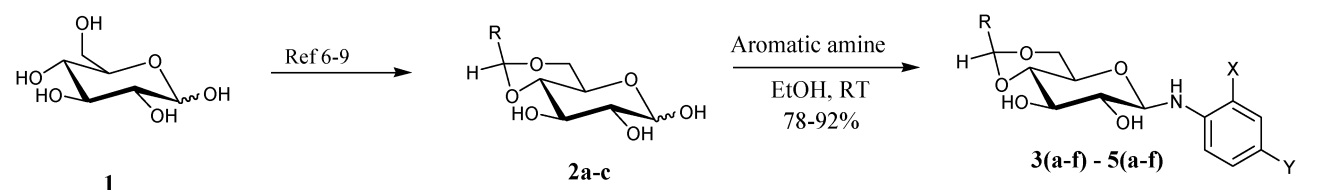
(BzGP) **2c** were synthesised from D-glucose (**1**)^{6–9} and characterised by adopting literature procedures. *N*-Glycosylamines were synthesised by reacting the primary amine in the aromatic moiety and the active hydroxyl group of the 4,6-*O*-protected D-glucose.^{10–12} *N*-Glycosylamine compounds (**3–5**) were identified through spectral techniques. During the synthesis of different *N*-glycosylamines using partially-protected saccharides, gel formation was observed and this observation prompted us to study the gelation property. ¹H NMR spectra of *N*-glycosylated products **3–5** showed glycosidic NH at around 5.0–6.0 ppm, the anomeric proton at around 4.5 ppm and the acetal proton changing with respect to the protecting group, whereas in the case of **3f**, **4f** and **5f**, the glycosidic NH appeared below 5.0 ppm. The existence of the β -anomeric form was identified from coupling constant values given in Table 1.

Gelation studies

All gel samples were prepared by dissolving the gelator in a solvent in such a way that it forms a homogenous solution. The solution was allowed to cool down to room temperature, whereby the gel is formed. The gelation ability of *N*-glycosylamines [**3(a–f)–5(a–f)**] has been assessed by using “stable to inversion of the container” method. The study includes eighteen substituted aromatic-based saccharide derivatives [**3(a–f)–5(a–f)**] in fourteen different organic solvents and the results of gelation are summarised in Table 2. Recently, we have reported⁴ the gelation of a novel class of 4,6-*O*-protected- β -C-glycosides and sugar-pyridyl derivatives and the present studies show gel formation of *N*-glycosylamines. In general, protecting groups such as ethylidene, butylidene and benzylidene present on the D-glucose moiety and the substituents present on the aromatic ring showed remarkable changes to the gelation process. Among the three different

^a Department of Organic Chemistry, University of Madras, Guindy Campus, Chennai—600 025, India.
E-mail: tmdas_72@yahoo.com; Fax: +91 44-22352494;
Tel: +91 44-22202814

^b Chemical Laboratory, Central Leather Research Institute (CSIR), Adyar, Chennai-600 020, India

Table 1 Synthesis of *N*-glycosylamines


R	Compound	Substituents		CGC %/g mL ⁻¹	δ (ano-H), $^3J_{H1,H2}$ /Hz	δ (gly-NH), $^3J_{H1,H2}$ /Hz	Yield (%)
		X	Y				
C ₃ H ₇ 3	a	H	Cl	1.5	4.51, 8.4	5.71, 6.9	89
	b	H	F	1.0	4.47–4.59, —	5.33, 6.3	81
	c ^a	F	H	—	4.52–4.56, —	5.63, 5.1	78
	d ^a	Cl	H	—	4.60, 8.4	5.59, —	92
	e	H	Br	1.5	4.50, 7.5	5.84, 6.9	85
	f ^a	CH ₃	H	—	4.56–4.63	4.56–4.63	91
CH ₃ 4	a	H	Cl	1.3	4.51, 8.4	5.60, 6.6	85
	b	H	F	1.5	4.47, 7.2	5.22, 6.6	86
	c	F	H	1.1	4.59, 5.1	5.93–5.95	81
	d ^a	Cl	H	—	4.60–4.74, —	5.60, 7.2	87
	e	H	Br	1.5	4.77, 5.1	5.68, 6.6	84
	f ^a	CH ₃	H	—	4.60, 7.4	4.68, 6.0	87
C ₆ H ₅ 5	a ^a	H	Cl	—	5.36, 6.3	5.54, —	81
	b	H	F	1.5	5.54, 6.6	5.51, —	83
	c	F	H	1.5	4.66, 8.8	5.99, 6.0	79
	d	Cl	H	1.5	4.69, 8.5	5.63, 7.3	91
	e	H	Br	2.0	4.56, 7.5	6.10, 6.6	89
	f ^a	CH ₃	H	—	5.54, 8.7	4.63–4.75	92

^a Denotes compound does not form gel. For all gelators, except gelators **4b**, **4c** and **4e**, 1,2-dichlorobenzene was used to measure the CGC. For **4b** and **4c**, *o*-xylene was used and for **4e** benzene was used.

4,6-*O*-protected *N*-glycosylamines studied, BGP and EGP derivatives possessing a halogen at the *para* position form gels in both polar and non-polar solvents. Whereas in case of BzGP, both *ortho*- and *para*-halogen substituted derivatives form gels. The difference in gelation ability is mainly due to the effect of the protecting group and it is as follows: **4c** > **5c** > **3a**, **3b**, **3e**, **4a**, **4b**, **4e** > **5b**, **5d**, **5e**. The critical gelation concentrations (CGC) of these compounds are given in Table 1. Among the various polar and non-polar solvents used for gelation, aromatic solvents *viz.*, 1,2-dichlorobenzene (1,2-DCB), *o*-xylene, *m*-xylene, benzene and toluene were found to be the best solvents for the gelation process, which may be attributed to a strong solute–solvent interaction. Of all the gelators, *N*-glycosylamine **3b** acts as an efficient organogelator and gels at lower concentrations (CGC: 1%). The gelation ability of the organogelator has a significant dependence on the protecting group and the substituents present on the aromatic ring. The greater gelation ability of BGP and EGP is due to higher London dispersion forces¹³ which exist between the alkyl chain groups. However, in BzGP, π – π interactions seem to be largely responsible for the gelation property. These results support the fact that partially protected *N*-glycosylamines with halogen substituted at the *para* position of the aromatic ring have a greater ability to undergo gelation compared to the substituents present at the *ortho* position. Moreover, anisotropic interactions through H-bonding, CH– π , π – π stacking and dipole–dipole interactions were also responsible for the linear aggregation of LMOGs, allowing gel formation. A pictorial representation of the groups in different

N-glycosylamines, which are responsible for gel formation is shown in Fig. 1.

Single crystal X-ray diffraction (XRD) data of compounds **3d**¹¹ and **4d**¹² helps us to understand the π – π stacking and H-bonding interactions that exists in different *N*-glycosylamines. Free hydroxyl groups present at the C-2 and C-3 positions of the glucopyranose ring are involved in the strong hydrogen

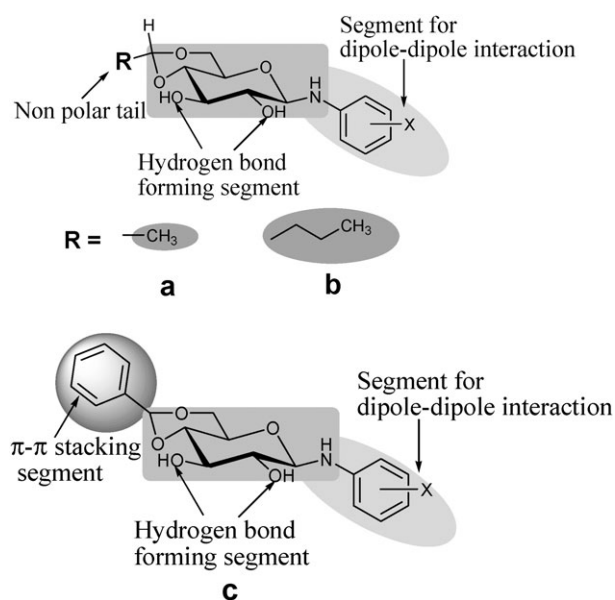
**Fig. 1** Rationalization of different groups responsible for gelation in different *N*-glycosylamines.

Table 2 Gelation studies of *N*-glycosylamines

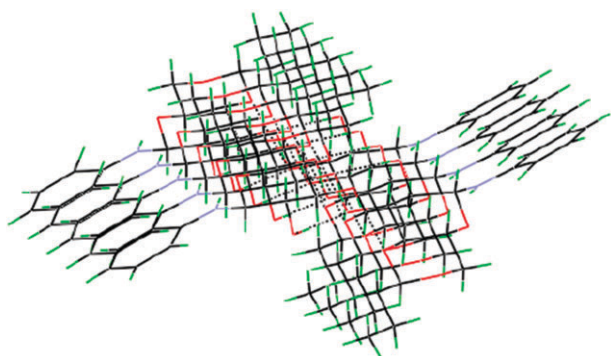
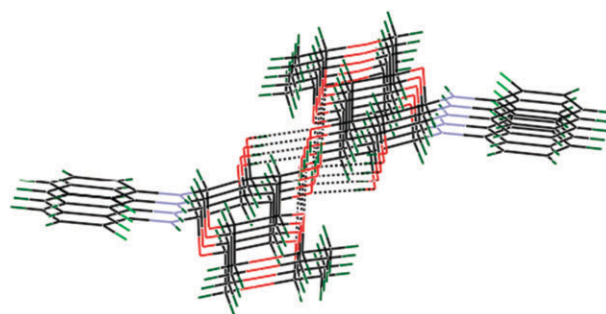
Solvent	3 (R = C ₃ H ₇)			4 (R = CH ₃)				5 (R = C ₆ H ₅)				
	a	b	e	a	b	c	e	b	c	d	e	
C ₆ H ₆	G	I	G	G	G	PG	G	G	PG	G	G	
CH ₃ C ₆ H ₅	G	P	G	G	G	G	G	G	G	G	S	
NO ₂ C ₆ H ₅	G	G	S	S	S	G	G	S	PG	S	S	
<i>p</i> -Xylene	G	G	G	PG	S	G	PG	G	G	G	G	
<i>o</i> -Xylene	G	G	G	PG	G	G	PG	PG	G	G	G	
<i>m</i> -Xylene	G	G	G	G	G	G	PG	PG	G	G	G	
1,2-DCB	G	G	G	G	PG	G	G	G	G	G	G	
CHCl ₃	P	P	S	S	G	S	S	S	S	S	P	
CCl ₄	P	P	G	PG	PG	PG	S	S	PG	G	G	
<i>i</i> -PrOH	G	G	PG	S	S	S	S	S	S	S	S	
1,2-DCE	P	G	P	G	G	PG	PG	PG	S	S	P	
CH ₃ CN	S	G	S	S	S	S	S	S	P	P	S	
MeOH	S	P	S	S	S	P	P	P	S	S	PG	
EtOH	S	P	S	S	S	PG	P	P	PG	S	S	

Note: G—gelator, PG—partial gelator, S—solution, P—precipitation, I—insoluble.

bonding, thereby forming a chain of molecules (Fig. 2 and Fig. 3). Although protecting groups are different in **3d** and **4d**, the hydrogen bonding interactions are the same and one may presume that just changing the protecting group and substituents may not affect the hydrogen bonding. However, H-bonding of the core sugar moiety remains unaltered in all the *N*-glycosylamines. Thus, self-assembly of a gelator molecule depends upon the nature of the protecting group and also the substituents present in the aromatic ring.

Microscopy studies

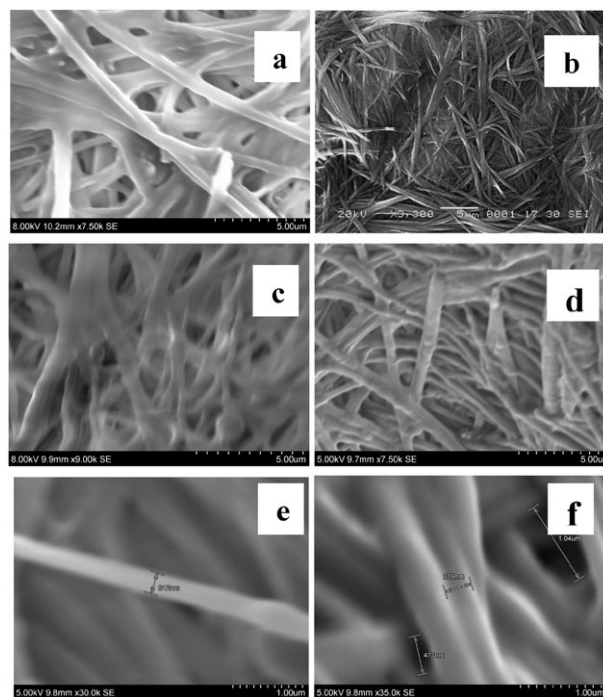
In order to obtain visual insight into the aggregation modes, scanning electron microscopy (SEM) images were obtained, showing the presence of elongated nanofibers (Fig. 4). SEM images of *N*-glycosylamines show well-defined 3D fibrous networks. SEM images of compound **3b** show the presence of intertwined thin sheets (Fig. 4b), whereas compounds **4e** and **5d** show elongated nanofibers around 310–350 nm with a bore size range of 400–1000 nm. SEM images of compound **5c** show it forms a fibrous network with junction points (Fig. 4c). From the SEM images (Fig. 4), the bore size of compound **3b** (CGC: 1%) is greater than that of **5c**, **5d** and **4e** (CGC: 1.5%), hence, compound **3b** acts as a good gelator, compared to the others. Three dimensional fibrous networks hold the solvent molecules together, which is due to the

**Fig. 2** π - π Stacking and H-bonding interactions of compound **3d**.¹¹**Fig. 3** π - π Stacking and H-bonding interactions of compound **4d**.¹²

existence of surface tension in the gels. In addition, the presence of a channel-like architecture with different bore size is responsible for the gelation capacities.

Thermoanalysis

To study the thermal properties of the organogelators and gels, differential scanning calorimetry (DSC) experiments for three different *N*-glycosylamines of 4,6-*O*-protected derivatives (**3a**, **4b** and **5c**) were performed. In the case of **3a**, the enthalpy values and the melting point peak values are found to be 191 J g⁻¹ and 189 °C, and 248 J g⁻¹ and 82 °C in the solid and gel phases, respectively (Fig. 5). The enthalpy values and the melting point peaks for compound **4b** are 35 J g⁻¹ and 128 °C in the solid phase, and 74 J g⁻¹ and 99 °C in the gel phase. The peak appearing at around 112 °C ($\Delta H = 138$ J g⁻¹) is due to the liberation of moisture. The enthalpy values and melting point peak for compound **5c** and its gel were found to be 113.4 J g⁻¹ and 143 °C, and 186 J g⁻¹

**Fig. 4** SEM images of organogel formed from (a), **5d** in 1,2-DCB; (b), **3b** in 1,2-DCE; (c), **5c** in 1,2-DCB; (d), **4e** in benzene; (e), **4e** in benzene (magnified) and (f), **4e** in benzene (fiber and bore are labeled).

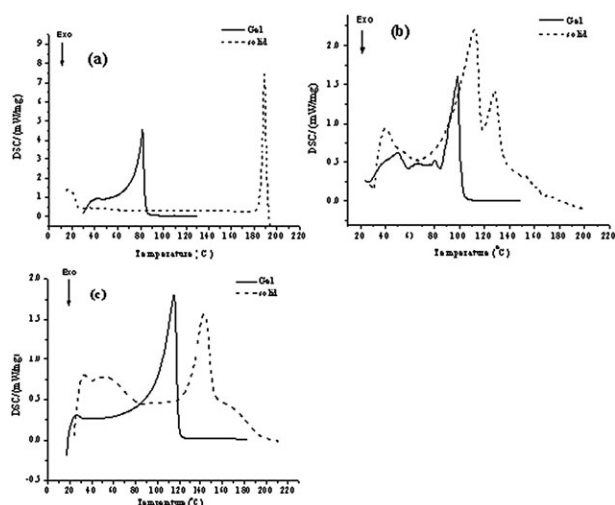


Fig. 5 DSC spectra of (a) **3a** (gel formed from benzene), (b) **4b** (gel formed from 1,2-DCE) and (c) **5c** (gel formed from toluene).

and 115 °C, respectively. These results indicate the thermal stabilities of both gel and organogelator. DSC studies further reveal that in the gel phase, the molecules were loosely packed and the system moves from the most ordered state to a less ordered state. The phase transition temperatures of compounds, **3a**, **4b** and **5c** and their corresponding gels are given in Table 3. The melting temperatures of gelator and gel are obtained from DSC experiments.

NMR studies

^1H NMR studies were carried out for solution of 1.0–1.5% wt of compounds **4a** and **4f**. In the case of compound **4a** (Fig. 6) the formation of the gel at 27 °C was accompanied by a broadening and shifting of both aromatic and core sugar proton signals. The ^1H NMR spectrum of non-gelator **4f** shows slight broadening due to D_2O exchange and not due to gelation (Fig. 7); gelator molecules are assembled in the gel network by means of hydrogen bonding, π - π stacking and dipole-dipole interactions, which results in the broadening of signals and due to long correlation times. The entire broadening and shifting of signals in the organogelator **4a** shows the involvement of the aromatic ring, the sugar part and also the protecting group, whereas, in the case of non-gelator molecule **4f**, these effects were not observed. Moreover, the involvement of H-bonding in gelation can also be explained by FT-IR and single crystal XRD studies.^{11,12}

FT-IR studies

The role of hydrogen bonding in the process of gelation was established with the help of FT-IR studies. In order to explain the H-bonding, we have measured the FT-IR spectra of

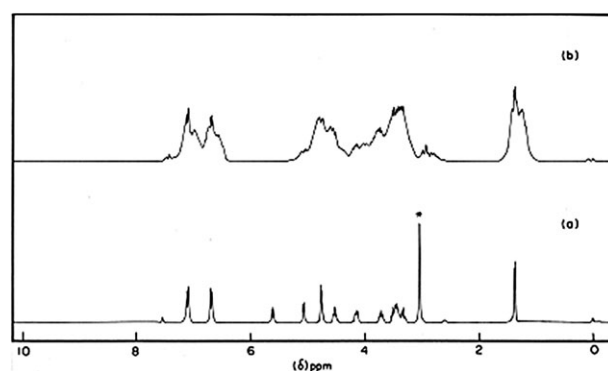


Fig. 6 ^1H NMR of compound, **4a** recorded at 27 °C in (a) CDCl_3 + 2 drops of $\text{DMSO}-d_6$ and (b) CDCl_3 + 2 drops of $\text{DMSO}-d_6$ + 4 drops of D_2O .

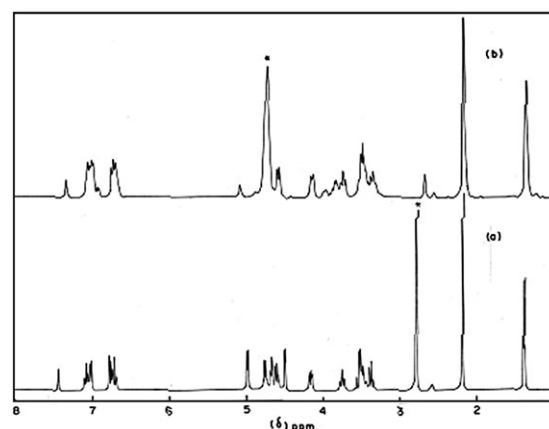


Fig. 7 ^1H NMR of compound, **4f** recorded at 27 °C in (a) CDCl_3 + 2 drops of $\text{DMSO}-d_6$ and (b) CDCl_3 + 2 drops of $\text{DMSO}-d_6$ + 4 drops of D_2O .

N-glycosylamines both in solid and gel phase. FT-IR spectra of the gel prepared from **3d** in 1,2-DCB shows five prominent characteristic peaks corresponding to ν_{NH} and ν_{OH} which appear at 3578, 3446, 3352, 3235 and 3066 cm^{-1} (Fig. 8). The degree of H-bonding was determined from the relative intensities of the well known $-\text{OH}$ stretching vibration at around 3600 cm^{-1} which corresponds to free $-\text{OH}$ and at 3300 cm^{-1} which corresponds to bonded $-\text{OH}$.¹⁴ The decrease in intensity of the peak at 3578 cm^{-1} and the appearance of the strong peaks at 3352, 3235 and 3066 cm^{-1} in the gel show the presence of bonded $-\text{OH}$. However, in the solid, all four peaks corresponding to the $-\text{OH}$ group merged and appeared as a broad band with shoulders at around 3355 cm^{-1} . In compound **5d**, there is a prominent shift in wavelength between gel and gelator, which clearly indicates the presence of hydrogen bonding as shown in Fig. 8.

Table 3 Melting temperatures of **3a**, **4b** and **5c** in the solid and gel phases

Compound	Phase transition temperature of gelator/°C	Phase transition temperature of gel/°C
3a	189	82
4b	128	99
5c	143	115

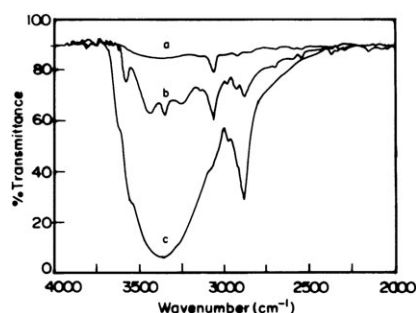


Fig. 8 FT-IR spectra of (a), gelator solvent (1,2-DCB); (b), **5d** (gel formed from 1,2-DCB) and (c), **5d** (solid in KBr matrix).

Computational studies

In the present study, gelators **3b**, **4b** and **5b** and non-gelators **3f**, **4f**, and **5f** have been taken into account. All the systems were optimized (without any geometrical constraint) by using the M05-2X hybrid density functional method.¹⁵ The optimized geometries were characterized as the minima on the potential energy surface by frequency analysis. The stabilization energies (SEs) are obtained using the equation,

$$SE = -[(E_{\text{complex}} - (E_{\text{monomer1}} + E_{\text{monomer2}}))]$$

where E_{complex} , E_{monomer1} , and E_{monomer2} are the total energies of the complex and the monomers. The SE are corrected for basis set superposition error (BSSE) using the method adopted by Boys and Bernardi.¹⁶ All the calculations were performed using the GAUSSIAN 03 (revision E.01) suite of programs.¹⁷ Due to the large system size and limited computational facility, two approaches were used for calculation here: (i) the complete system with the 6-31G* basis set; (ii) only the active part of the system with the 6-311++G* basis set.

All the optimized dimeric complexes are shown in Fig. 9 and their corresponding BSSE-corrected SE are depicted in Table 4. Since the binding energies for gelator complexes are comparatively larger than those of non-gelators, one can predict that the dipole–dipole interactions (Fig. 9) play a vital role in the gel formation. Fluorine substitution plays a significant role in the high SE values because it interacts with the glycosidic NH group of *N*-glycosylamines. In the case of non-gelators, very weak CH– π interactions are observed, causing the lower SE.

Other interactions are also important in gel formation, therefore analysis of just the active part of the system has been considered. Since this system size is small, a larger basis set has been employed for the calculations. All the SE and optimized geometries are shown in Table 5 and Fig. 10. In the case of the benzene dimer (Bz–Bz), only the stable parallel-displaced conformation is taken into account, the other conformation, parallel, is less stable.^{4b} The calculation suggests that, apart from the dipole–dipole interacting sites, various other possible interactions play a significant role in the gel formation (Fig. 10). The Bz–Bz stacking energy is 1.67 kcal mol^{−1} which reflects in the weak tail–tail interactions in **5b**, whereas in the case of **3b** and **4b**, head–head and head–tail interactions were observed. Two different basis sets were used here, but in the first case (*i.e.* complete system consideration) results show good agreement with the

experimental results. Moreover, *cis*-Me–C₆H₄–NH₂ and *cis*-F–C₆H₄–NH₂ have larger SE values than their corresponding *trans* arrangements, as presented in Table 5, but practically (*i.e.* considering the complete molecule) this arrangement is highly unstable due to the repulsion among the various groups.

Conclusion

In summary, we have reported the synthesis and gelation properties of various sugar-based *N*-glycosylamines derived from aromatic amines. The presence of π – π stacking and H-bonding in *N*-glycosylamines was identified from single crystal XRD studies.^{11,12} The gelation nature of these sugar *N*-glycosylamine derivatives depends on the protecting groups such as 4,6-*O*-butylidene, 4,6-*O*-ethylidene, 4,6-*O*-benzylidene and halogen substituents. Variation in the protecting groups and the position of the halogen atom alters the morphology and the gelation abilities to a considerable extent as observed from SEM analysis. Thermoanalysis of these gelators reveals that molecules move from the most ordered state to a less ordered state by forming a gel, whereby the melting temperature becomes lower than the corresponding gelator. Moreover, the presence of H-bonding was established from FT-IR and of molecular aggregation by NMR studies. Computational studies show the existence of dipole–dipole interactions, CH– π and π – π stacking which play a vital role in gel formation. Experimental results were reinforced with theoretical prediction. From these results, even a small tuning of molecules can drastically alter their gelation properties. Based on the present studies, one could conclude that the presence of aliphatic or aromatic rings present at the 4,6-*O*-positions of the D-glucose unit of *N*-glycosylamines result in gelation. The presence of halogen atoms is needed for dipole–dipole interaction, whereas the methyl-substituted do not form gels.

Experimental

General details

All reagents were purchased from Sigma Aldrich (benzaldehyde dimethyl acetal), SRL (D-glucose) and Loba chemie (butyraldehyde, paraldehyde, aromatic amines). Solvents used for gelation studies were analytical grade and were purchased from Qualigens, Sd-fine chemicals and SRL, India. NMR spectra were recorded with a Bruker Avance 300 (300 MHz) using TMS as internal standard. FT-IR studies were carried out using a Perkin Elmer PE257 IR spectrometer. Thermal transitions for gelators and gels were determined on a NETZSCH DSC 204 instrument. The measurements were carried out under nitrogen atmosphere using 50 μ L sealed aluminium sample pans. The temperature calibration for the DSC was done using two standard materials (n-decane, indium) and energy calibration by an indium standard (28.45 J g^{−1}). The gels were imaged with a HITACHI-S-3400W scanning electron microscope. The samples were gold-coated in such a way that the gold coating was less than 1 nm thick on average. Elemental analysis was performed by using a Perkin-Elmer 2400 series CHNS/O analyser.

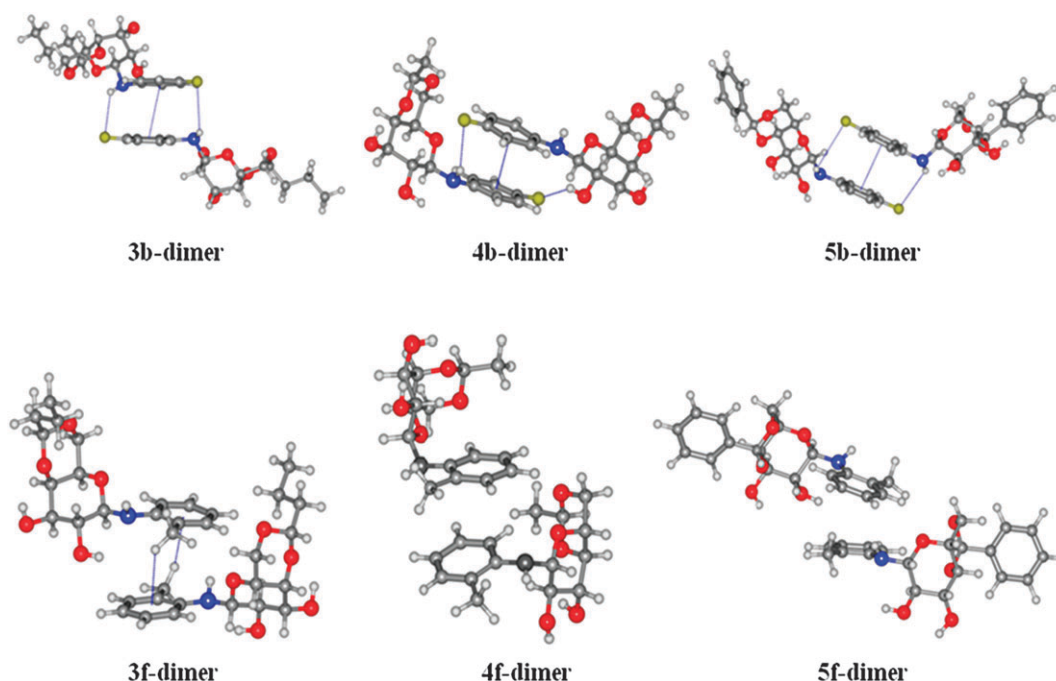


Fig. 9 Optimized geometries of the complete dimer: grey = C, blue = N, red = O, white = H, yellow = F

Table 4 Stabilization energy due to dipole interactions obtained at the M05-2X level of calculation using 6-31G* basis set

S. No.	Compound	BSSE-corrected SE/kcal mol ⁻¹
1	3b	9.66948
2	4b	6.98644
3	5b	8.39269
4	3f	2.54499
5	4f	1.52937
6	5f	3.25684

BGP, EGP and BzGP were synthesised by adopting the literature procedures.^{6–9} *N*-Glycosylamines **3c**, **3d**, **4c**, **4d**, **5c** and **5d** were synthesised and their purity confirmed using different spectral techniques.^{10–12} Synthetic procedures and spectral data for all other compounds are provided below.

Synthesis

General synthetic procedure for the synthesis of compounds **3–5** is as follows:

To a solution of 1 mol of the 4,6-*O*-protected-β-D-glucopyranose, (**2a–c**) in 10 ml of ethanol, 1.2 mol of the substituted aniline was added. The reaction mixture was then stirred at 50 °C for 10 min and at room temperature for 24 h. The reaction was thereby followed through TLC. The solid, which separates, was filtered off, washed with ethanol and dried using diethyl ether.

Synthesis of gels

The gelation ability of *N*-glycosylamines was determined by the “stable to inversion of the container” method.¹³ The gelation properties have been tested with fourteen different solvents as follows: gelator (1.5 mg) was mixed in a close capped test tube with 1 ml of solvent to result in a

concentration of 1.5% (gm L⁻¹) and the mixture was heated until the solid was dissolved. By this procedure, the solvent boiling point becomes higher than that under standard atmospheric pressure. The sample vial was cooled in air to 25 °C, left for 12 h at this temperature and then turned upside down. When the gelator formed a clear or slightly opaque gel by immobilizing the solvent at this stage, it was denoted by “G”. Some of them form a partial gel, denoted PG. Some of them are insoluble and some get precipitated, denoted by I and P, respectively.

Spectral characterization of gelators

Abbreviations, such as Sac and Ar, correspond to the saccharide and aromatic groups, respectively.

4,6-*O*-Butylidene-*N*-(*p*-chlorophenyl)-β-D-glucopyranosylamine (3a**).** Mp 186–188 °C; ¹H NMR (CDCl₃ + DMSO-*d*₆): δ 7.09 (d, *J* = 8.4 Hz, 2H, Ar-H), 6.68 (d, *J* = 8.4 Hz, 2H, Ar-H), 5.71 (d, *J* = 6.9 Hz, 1H, -NH), 5.10 (s, 1H, Sac-OH), 4.80 (s, 1H, Sac-OH), 4.57 (d, *J* = 4.8 Hz, 1H, Sac-H), 4.51 (t, *J* = 8.4 Hz, 1H, Sac-H), 4.12–4.16 (dd, *J* = 3.9 Hz, *J* = 9.6 Hz, 1H, Sac-H), 3.69 (t, *J* = 8.7 Hz, 1H, Sac-H), 3.26–3.51 (m, 4H, Sac-H), 1.60–1.67 (m, 2H, -CH₂), 1.37–1.50 (m, 2H, -CH₂), 0.92 (t, *J* = 7.2 Hz, 3H, -CH₃) ppm; ¹³C NMR (CDCl₃ + DMSO-*d*₆): δ 144.7, 128.3, 122.4, 114.6, 101.7, 86.2, 80.0, 73.6, 73.4, 67.9, 66.7, 35.8, 16.9, 13.5 ppm. Anal. calcd for C₁₆H₂₂NO₅Cl: C 55.90, H 6.45, N 4.07. Found C 56.18, H 6.62, N 4.19.

4,6-*O*-Butylidene-*N*-(*p*-fluorophenyl)-β-D-glucopyranosylamine (3b**).** Mp 147–149 °C; ¹H NMR (CDCl₃ + DMSO-*d*₆): δ 6.84–6.90 (m, 2H, Ar-H), 6.67–6.71 (m, 2H, Ar-H), 5.33 (d, *J* = 6.3 Hz, 1H, -NH), 4.99 (d, *J* = 4.2 Hz, 1H, Sac-H), 4.47–4.59 (m, 3H, Sac-H), 4.14–4.19 (dd, *J* = 4.2 Hz, *J* = 9.6 Hz,

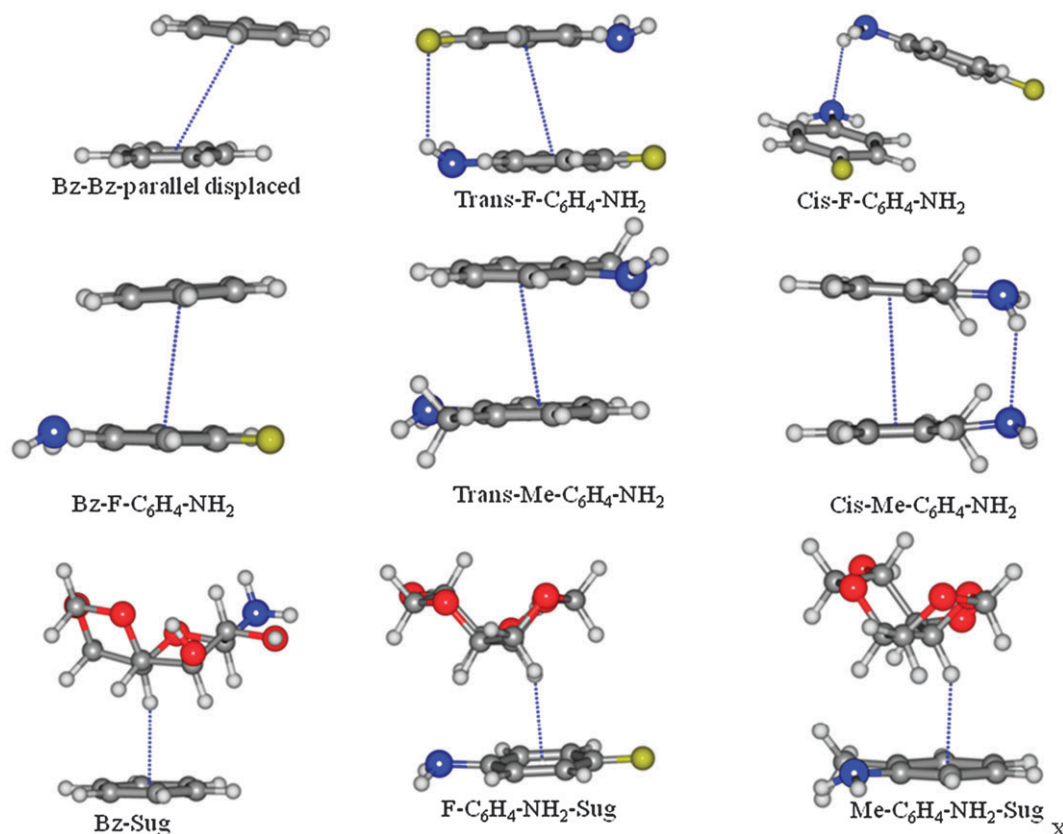


Fig. 10 Optimized geometries of the various interacting active parts of the gelators and non-gelators: grey = C, blue = N, red = O, white = H, yellow = F.

1H, Sac-H), 3.69–3.73 (m, 1H, Sac-H), 3.28–3.54 (m, 4H, Sac-H), 1.61–1.67 (m, 2H, $-\text{CH}_2$), 1.41–1.48 (m, 2H, $-\text{CH}_2$), 0.92 (t, $J = 6.9$ Hz, 3H, $-\text{CH}_3$) ppm; ^{13}C NMR ($\text{CDCl}_3 + \text{DMSO}-d_6$): δ 142.5, 115.4, 115.1, 114.8, 114.7, 102.1, 87.3, 80.3, 74.1, 73.9, 68.3, 67.1, 36.1, 17.2, 13.8 ppm. Anal. calcd for $\text{C}_{16}\text{H}_{22}\text{NO}_5\text{F}$: C 58.71, H 6.77, N 4.28. Found C 58.47, H 7.06, N 4.51.

4,6-*O*-Butylidene-*N*-(*p*-bromophenyl)- β -D-glucopyranosylamine (3e). Mp 118–120 °C; ^1H NMR ($\text{CDCl}_3 + \text{DMSO}-d_6$): δ 7.21 (d, $J = 8.7$ Hz, 2H, Ar-H), 6.64 (d, $J = 8.7$ Hz, 2H, Ar-H), 5.84 (d, $J = 6.9$ Hz, 1H, $-\text{NH}$), 5.22 (d, $J = 4.2$ Hz, 1H, Sac-H), 4.95 (d, $J = 3.3$ Hz, 1H, Sac-H), 4.56 (t, $J = 5.1$ Hz, 1H, Sac-H), 4.50 (d, $J = 7.5$ Hz, 1H, Sac-H), 4.11–4.15 (dd, $J = 4.2$ Hz, $J = 9.4$ Hz, 1H, Sac-H), 3.65–3.72 (m, 1H, Sac-H), 3.29–3.50 (m, 4H, Sac-H), 1.59–1.67 (m, 2H, $-\text{CH}_2$), 1.37–1.49 (m, 2H, $-\text{CH}_2$), 0.92 (t, $J = 7.3$ Hz, 3H, $-\text{CH}_3$) ppm;

^{13}C NMR ($\text{CDCl}_3 + \text{DMSO}-d_6$): δ 145.1, 131.1, 115.1, 109.5, 101.7, 90.0, 80.04, 73.6, 73.4, 67.9, 66.7, 35.8, 16.9, 13.5 ppm. Anal. calcd for $\text{C}_{16}\text{H}_{22}\text{NO}_5\text{Br}$: C 49.50, H 5.71, N 3.61. Found C 49.27, H 5.92, N 3.45.

4,6-*O*-Butylidene-*N*-(*o*-methylphenyl)- β -D-glucopyranosylamine (3f). Mp 101–103 °C; ^1H NMR ($\text{CDCl}_3 + \text{DMSO}-d_6$): δ 7.01–7.11 (m, 2H, Ar-H), 6.69–6.78 (m, 2H, Ar-H), 4.56–4.63 (m, 3H, Sac-H), 4.15–4.19 (dd, $J = 4.2$ Hz, $J = 9.2$ Hz, 1H, Sac-H), 3.73–3.79 (m, 1H, Sac-H), 3.41–3.55 (m, 3H, Sac-H), 3.34 (t, $J = 8.9$ Hz, 1H, Sac-H), 3.03 (s, 2H, Sac-H), 2.19 (s, 3H, Ar- CH_3), 1.62–1.68 (m, 2H, $-\text{CH}_2$), 1.41–1.48 (m, 2H, $-\text{CH}_2$), 0.92 (t, $J = 7.4$ Hz, 3H, $-\text{CH}_3$) ppm; ^{13}C NMR ($\text{CDCl}_3 + \text{DMSO}-d_6$): δ 143.5, 129.7, 126.5, 122.4, 118.4, 111.4, 101.8, 86.1, 79.9, 73.8, 73.6, 68.0, 66.8, 35.8, 17.0, 16.87, 13.4 ppm. Anal. calcd for $\text{C}_{17}\text{H}_{25}\text{NO}_5$: C 63.14, H 7.79, N 4.33. Found C 62.89, H 7.87, N 4.50.

Table 5 Stabilization energies due to all possible interactions obtained from M05-2X level of calculation using the 6-311++G* basis set

Entry	Interacting species	Nature of interaction	BSSE-corrected SE/kcal mol $^{-1}$
1	Bz (parallel displaced)	Dimer	1.6739
2	<i>trans</i> -Me-C ₆ H ₄ -NH ₂	Dimer	3.3971
3	<i>cis</i> -Me-C ₆ H ₄ -NH ₂	Dimer	5.8217
4	<i>trans</i> -F-C ₆ H ₄ -NH ₂	Dimer	5.1062
5	<i>cis</i> -F-C ₆ H ₄ -NH ₂	Dimer	6.8986
6	Bz-F-C ₆ H ₄ -NH ₂	—	2.8867
7	Bz-Sug	—	4.7878
8	F-C ₆ H ₄ -NH ₂ -Sug	—	5.9550
9	Me-C ₆ H ₄ -NH ₂ -Sug	—	6.8595

4,6-*O*-Ethylidene-*N*-(*p*-chlorophenyl)- β -D-glucopyranosylamine (4a). Mp 123–125 °C; ^1H NMR (CDCl_3 + $\text{DMSO}-d_6$): δ 7.09 (d, J = 8.7 Hz, 2H, Ar-H), 6.71 (d, J = 8.7 Hz, 2H, Ar-H), 5.60 (d, J = 6.6 Hz, 1H, -NH), 5.06 (d, J = 3.9 Hz, 1H, Sac-H), 4.74 (t, J = 4.0 Hz, 2H, Sac-H), 4.48–4.53 (dd, J = 6.9 Hz, J = 8.4 Hz, 1H, Sac-H), 4.11–4.16 (dd, J = 4.2 Hz, J = 9.9 Hz, 1H, Sac-H), 3.67–3.74 (m, 1H, Sac-H), 3.40–3.53 (m, 4H, Sac-H), 1.36 (d, J = 5.1 Hz, 3H, -CH₃) ppm; ^{13}C NMR (CDCl_3 + $\text{DMSO}-d_6$): δ 149.8, 133.6, 127.8, 119.8, 104.2, 91.5, 85.2, 78.9, 78.7, 73.0, 71.8, 25.2 ppm. Anal. calcd for $\text{C}_{14}\text{H}_{18}\text{NO}_5\text{Cl}$: C 53.25, H 5.75, N 4.44. Found C 53.46, H 5.63, N 4.61.

4,6-*O*-Ethylidene-*N*-(*p*-fluorophenyl)- β -D-glucopyranosylamine (4b). Mp 124–126 °C; ^1H NMR (CDCl_3 + $\text{DMSO}-d_6$): δ 6.85–6.90 (d, J = 8.6 Hz, 2H, Ar-H), 6.67–6.72 (d, J = 8.5 Hz, 2H, Ar-H), 5.22 (d, J = 6.6 Hz, 1H, -NH), 5.01 (d, J = 3.9 Hz, 1H, Sac-H), 4.73–4.76 (m, 2H, Sac-H), 4.49–4.45 (t, J = 7.2 Hz, 1H, Sac-H), 4.14–4.17 (m, 1H, Sac-H), 3.73–3.75 (m, 1H, Sac-H), 3.35–3.53 (m, 4H, Sac-H), 1.38 (d, J = 5.1 Hz, 3H, -CH₃) ppm; ^{13}C NMR (CDCl_3 + $\text{DMSO}-d_6$): δ 147.4, 120.3, 120.0, 119.6, 119.5, 104.1, 92.6, 85.2, 78.99, 78.7, 73.1, 71.8, 25.2 ppm. Anal. calcd for $\text{C}_{14}\text{H}_{18}\text{NO}_5\text{F}$: C 56.18, H 6.06, N 4.68. Found C 55.87, H 6.24, N 4.75.

4,6-*O*-Ethylidene-*N*-(*p*-bromophenyl)- β -D-glucopyranosylamine (4c). Mp 127–129 °C; ^1H NMR (CDCl_3 + $\text{DMSO}-d_6$): δ 7.26 (d, J = 8.7 Hz, 2H, Ar-H), 6.62 (d, J = 8.7 Hz, 2H, Ar-H), 5.68 (d, J = 6.6 Hz, 1H, -NH), 5.20 (d, J = 3.9 Hz, 1H, Sac-H), 4.84 (d, J = 3.4 Hz, 1H, Sac-H), 4.77 (d, J = 5.1 Hz, 1H, Sac-H), 4.52–4.58 (t, J = 7.8 Hz, 1H, Sac-H), 4.15–4.19 (dd, J = 4.2 Hz, J = 10.2 Hz, 1H, Sac-H), 3.32–4.19 (m, 5H, Sac-H), 1.40 (d, J = 4.8 Hz, 3H, -CH₃); ^{13}C NMR (CDCl_3 + $\text{DMSO}-d_6$): δ 145.3, 131.6, 115.4, 110.1, 99.3, 80.2, 73.9, 73.7, 68.2, 66.9, 20.3. Anal. calcd for $\text{C}_{14}\text{H}_{18}\text{NO}_5\text{Br}$: C 46.68, H 5.04, N 3.89. Found C 46.45, H 5.26, N 4.03.

4,6-*O*-Ethylidene-*N*-(*o*-methylphenyl)- β -D-glucopyranosylamine (4f). Mp 129–131 °C; ^1H NMR (CDCl_3 + $\text{DMSO}-d_6$): δ 7.02–7.11 (m, 2H, Ar-H), 6.69–6.79 (m, 2H, Ar-H), 4.98 (d, J = 4.2 Hz, 1H, Sac-H), 4.73–4.78 (dd, J = 4.8 Hz, J = 9.9 Hz, 1H, Sac-H), 4.68 (d, J = 6.0 Hz, 1H, Sac-H), 4.60 (t, J = 7.4 Hz, 1H, Sac-H), 4.50 (d, J = 2.7 Hz, 1H, Sac-H), 4.15–4.19 (m, 1H, Sac-H), 3.73–3.79 (m, 1H, Sac-H), 3.50–3.57 (m, 4H, Sac-H), 2.19 (s, 3H, Ar-CH₃), 1.39 (d, J = 4.8 Hz, 3H, -CH₃) ppm; ^{13}C NMR (CDCl_3 + $\text{DMSO}-d_6$): δ 143.9, 130.1, 126.9, 122.8, 118.8, 111.8, 99.4, 86.3, 80.3, 74.3, 74.1, 68.3, 67.0, 20.3, 17.4 ppm. Anal. calcd for $\text{C}_{15}\text{H}_{21}\text{NO}_5$: C 61.00, H 7.17, N 4.74. Found C 61.13, H 7.36, N 4.60.

4,6-*O*-Benzylidene-*N*-(*p*-chlorophenyl)- β -D-glucopyranosylamine (5a). Mp 140–143 °C; ^1H NMR (CDCl_3 + $\text{DMSO}-d_6$): δ 7.51 (d, J = 3.3 Hz, 2H, Ar-H), 7.26 (d, J = 3.3 Hz, 3H, Ar-H), 7.12 (d, J = 8.4 Hz, 2H, Ar-H), 6.70 (d, J = 8.7 Hz, 2H, Ar-H), 5.54 (s, 1H, -NH), 5.36 (d, J = 6.3 Hz, 1H, Sac-H), 4.91 (s, 1H, Sac-OH), 4.56–4.61 (m, 2H, Sac-H), 4.28–4.33 (m, 1H, Sac-H), 3.59–3.84 (m, 5H, Sac-H) ppm; ^{13}C NMR (CDCl_3 + $\text{DMSO}-d_6$): δ 114.7, 137.3, 129.1, 128.9, 128.1, 126.4, 123.5, 115.2, 101.8, 86.8, 80.9, 74.1, 73.9, 68.8,

67.1 ppm. Anal. Calcd for $\text{C}_{19}\text{H}_{20}\text{NO}_5\text{Cl}$: C 60.40, H 5.34, N 3.71. Found C 60.65, H 5.19, N 3.94.

4,6-*O*-Benzylidene-*N*-(*p*-fluorophenyl)- β -D-glucopyranosylamine (5b). Mp 117–119 °C; ^1H NMR (CDCl_3 + $\text{DMSO}-d_6$): δ 7.46–7.51 (m, 2H, Ar-H), 7.34–7.36 (m, 3H, Ar-H), 6.82–6.90 (m, 2H, Ar-H), 6.69–6.73 (dd, J = 4.5 Hz, J = 11.4 Hz, 2H, Ar-H), 5.53 (m, 1H, -NH), 5.18 (s, 1H, Sac-OH), 4.48–5.04 (m, 2H, Sac-H), 5.54 (d, J = 6.6 Hz, 1H, Sac-H), 4.30–4.34 (m, 1H, Sac-H), 3.45–3.95 (m, 5H, Sac-H) ppm; ^{13}C NMR (CDCl_3 + $\text{DMSO}-d_6$): δ 142.4, 133.8, 132.9, 131.3, 120.3, 120.0, 119.6, 119.5, 106.4, 92.2, 86.0, 78.9, 78.6, 73.6, 71.8 ppm. Anal. calcd for $\text{C}_{19}\text{H}_{20}\text{NO}_5\text{F}$: C 63.15, H 5.58, N 3.88. Found C 62.80, H 5.77, N 3.71.

4,6-*O*-Benzylidene-*N*-(*p*-bromophenyl)- β -D-glucopyranosylamine (5c). Mp 135–137 °C; ^1H NMR (CDCl_3 + $\text{DMSO}-d_6$): δ 7.50 (d, J = 2.4 Hz, 2H, Ar-H), 7.35 (d, J = 2.9 Hz, 2H, Ar-H), 6.88 (d, J = 8.7 Hz, 2H, Ar-H), 7.22 (d, J = 8.7 Hz, 1H, Ar-H), 6.67 (d, J = 8.7 Hz, 1H, Ar-H), 6.10 (d, J = 6.6 Hz, 1H, -NH), 5.53 (d, J = 5.7 Hz, 1H, Sac-H), 4.56 (t, J = 7.5 Hz, 1H, Sac-H), 4.21–4.30 (m, 2H, Sac-H), 4.10 (d, J = 2.4 Hz, 1H, Sac-H), 3.12–3.72 (m, 5H, Sac-H) ppm; ^{13}C NMR (CDCl_3 + $\text{DMSO}-d_6$): δ 150.7, 142.6, 136.4, 133.8, 132.9, 131.4, 120.3, 114.3, 106.3, 91.3, 86.1, 83.4, 78.6, 73.6, 71.8 ppm. Anal. calcd for $\text{C}_{19}\text{H}_{20}\text{NO}_5\text{Br}$: C 54.04, H 4.77, N 3.32. Found C 54.36, H 4.71, N 3.42.

4,6-*O*-Benzylidene-*N*-(*o*-methylphenyl)- β -D-glucopyranosylamine (5f). Mp 99–101 °C; ^1H NMR (CDCl_3 + $\text{DMSO}-d_6$): δ 7.51 (d, J = 4.5 Hz, 2H, Ar-H), 7.36 (d, J = 3.9 Hz, 3H, Ar-H), 7.02–7.12 (m, 2H, Ar-H), 6.70–6.81 (m, 2H, Ar-H), 5.54 (d, J = 8.7 Hz, 1H, -NH), 5.02 (s, 1H, Sac-OH), 4.63–4.75 (m, 3H, Sac-H), 4.32–4.37 (m, 1H, Sac-H), 3.48–3.85 (m, 4H, Sac-H), 2.87 (m, 1H, Sac-H), 2.20 (s, 3H, Ar-CH₃) ppm; ^{13}C NMR (CDCl_3 + $\text{DMSO}-d_6$): δ 148.2, 141.6, 134.2, 133.1, 132.2, 131.0, 130.6, 126.9, 122.9, 116.0, 105.8, 91.0, 85.3, 78.3, 78.1, 73.0, 71.2, 21.6 ppm. Anal. calcd for $\text{C}_{20}\text{H}_{23}\text{NO}_5$: C 67.21, H 6.49, N 3.92. Found C 67.55, H 6.23, N 3.78.

Acknowledgements

T.M.D. acknowledges financial support from the Department of Science and Technology, New Delhi, India. We thank the Department of Science and Technology, New Delhi for the 300 MHz NMR facility under FIST scheme to the Department of Organic Chemistry, University of Madras, Chennai, India. S.N. thank UGC, New Delhi for research fellowship.

References

- (a) J. Peng, K. Liu, Q. Zhang, X. Feng and Y. Fang, *Langmuir*, 2008, **24**, 2992; (b) M. George, S. L. Snyder, P. Terech, C. J. Glinka and R. G. Weiss, *J. Am. Chem. Soc.*, 2003, **125**, 10275; (c) M. George and R. G. Weiss, *Chem. Mater.*, 2003, **15**, 2879; (d) X. Huang, P. Terech, S. R. Raghavan and R. G. Weiss, *J. Am. Chem. Soc.*, 2005, **127**, 4336; (e) X. Huang, S. R. Raghavan, P. Terech and R. G. Weiss, *J. Am. Chem. Soc.*, 2006, **128**, 15341; (f) M. George, G. P. Funkhouser and R. G. Weiss, *Langmuir*, 2008, **24**, 3537; (g) T. Klawonn, A. Gansauer, I. Winkler, T. Lauterbach, D. Franke, R. J. M. Nolte, M. C. Feiters, H. Borner, J. Hentschel and K. H. Dotz, *Chem. Commun.*, 2007,

- 1894; (h) L. A. Estroff and A. D. Hamilton, *Chem. Rev.*, 2004, **104**, 1201; (i) S. Bhattacharya and S. N. G. Acharya, *Chem. Mater.*, 1999, **11**, 3504; (j) M. de Loos, J. H. van Esch, R. M. Kellogg and B. L. Feringa, *Tetrahedron*, 2007, **63**, 7285; (k) M. George, G. Tan, V. T. Jhon and R. G. Weiss, *Chem.-Eur. J.*, 2005, **11**, 3243; (l) M. George and R. G. Weiss, *Acc. Chem. Res.*, 2006, **39**, 489; (m) C. Baddeley, Z. Yan, G. King, P. M. Woodward and J. D. Badjic, *J. Org. Chem.*, 2007, **72**, 7270; (n) A. Pal, Y. K. Ghosh and S. Bhattacharya, *Tetrahedron*, 2007, **63**, 7334; (o) K. Tanaka, S. Hayashi and M. R. Caira, *Org. Lett.*, 2008, **10**, 2119.
- 2 (a) O. Gronwald, K. Sakurai, R. Luboradzki, T. Kimura and S. Shinkai, *Carbohydr. Res.*, 2001, **331**, 307; (b) O. Gronwald and S. Shinkai, *J. Chem. Soc., Perkin Trans. 2*, 2001, **2**, 1933; (c) R. J. H. Hafkamp, B. P. A. Kokke, I. M. Danke, H. P. M. Geurts, A. E. Rowan, M. C. Feiters and J. M. Nottle, *Chem. Commun.*, 1997, 545; (d) R. Ghosh, A. Chakrabarty, D. K. Maiti and V. G. Puranik, *Org. Lett.*, 2006, **8**, 1061; (e) B. Xing, C.-W. Yu, K.-H. Chow, P.-L. Ho, D. Fu and B. Xu, *J. Am. Chem. Soc.*, 2002, **124**, 14846; (f) S. Kiyonaka, K. Sugiyasu, S. Shinkai and I. Hamachi, *J. Am. Chem. Soc.*, 2002, **124**, 10954; (g) J. H. Jung, J. A. Rim, E. J. Cho, S. J. Lee, I. Y. Jeong, N. Kameda, M. Masuda and T. Shimizu, *Tetrahedron*, 2007, **63**, 7449; (h) S. Cheuk, E. D. Stevens and G. Wang, *Carbohydr. Res.*, 2009, **344**, 417 and references cited therein.
- 3 (a) S. Zhang, *Nat. Biotechnol.*, 2003, **21**, 1171; (b) X. Y. Gao and H. Matsui, *Adv. Mater.*, 2005, **17**, 2037; (c) D. T. Bong, T. D. Clark, J. R. Granja and M. R. Ghadiri, *Angew. Chem., Int. Ed.*, 2001, **40**, 988; (d) V. Percec, A. E. Dulcey, V. S. K. Balagurusamy, Y. Miura, J. Smidrkal, M. Peterca, S. Nummelin, U. Edlund, S. D. Hudson, P. A. Heiney, H. Duan, S. N. Maganov and S. A. Vinogradov, *Nature*, 2004, **430**, 764.
- 4 (a) S. Nagarajan, T. Mohan Das, P. Arjun and N. Raaman, *J. Mater. Chem.*, 2009, **19**, 4587; (b) K. Karthik Kumar, M. Elango, V. Subramanian and T. Mohan Das, *New J. Chem.*, 2009, **33**, 1570; (c) S. Nagarajan and T. Mohan Das, *Carbohydr. Res.*, 2009, **334**, 1028.
- 5 K. Sugiyasu, S.-I. Kawano, N. Fujita and S. Shinkai, *Chem. Mater.*, 2008, **20**, 2863.
- 6 P. L. Barili, G. C. Berti, G. Catelani, C. Cini, F. D. Andran and F. Mastrorilli, *Carbohydr. Res.*, 1995, **278**, 43.
- 7 P. L. Mellies, C. L. Mehltrittter and E. C. Rist, *J. Am. Chem. Soc.*, 1951, **73**, 294.
- 8 G. T. Bonner, J. E. Bourne and D. Lewis, *J. Chem. Soc.*, 1965, 7453.
- 9 R. Barker and D. L. Mac Donald, *J. Am. Chem. Soc.*, 1960, **82**, 2301.
- 10 T. Mohan Das, C. P. Rao and E. Kolehmainen, *Carbohydr. Res.*, 2001, **334**, 261.
- 11 G. Rajsekhar, C. P. Rao, P. K. Saarenketo, E. Kolehmainen and K. Rissanen, *Carbohydr. Res.*, 2002, **337**, 187.
- 12 A. K. Sah, C. P. Rao, P. K. Saarenketo, E. K. Wegelius, K. Rissanen and E. Kolehmainen, *J. Chem. Soc., Dalton Trans.*, 2000, 3681.
- 13 H. Yu, H. Kawanishi and H. Koshima, *J. Photochem. Photobiol., A*, 2006, **178**, 62.
- 14 A. V. Stuart and G. B. B. M. Sutherland, *J. Chem. Phys.*, 1956, **24**, 559.
- 15 Y. Zhao, N. E. Schultz and D. G. Truhlar, *J. Chem. Theory Comput.*, 2006, **2**, 364.
- 16 S. F. Boys and F. Bernardi, *Mol. Phys.*, 1970, **19**, 553.
- 17 M. J. Frisch, G. W. Trucks, H. B. Schlegel, G. E. Scuseria, M. A. Robb, J. R. Cheeseman, J. A. Montgomery Jr, T. Vreven, K. N. Kudin, J. C. Burant, J. M. Millam, S. S. Iyengar, J. Tomasi, V. Barone, B. Mennucci, M. Cossi, G. Scalmani, N. Rega, G. A. Petersson, H. Nakatsuji, M. Hada, M. Ehara, K. Toyota, R. Fukuda, J. Hasegawa, M. Ishida, T. Nakajima, Y. Honda, O. Kitao, H. Nakai, M. Klene, X. Li, J. E. Knox, H. P. Hratchian, J. B. Cross, V. Bakken, C. Adamo, J. Jaramillo, R. Gomperts, R. E. Stratmann, O. Yazyev, A. J. Austin, R. Cammi, C. Pomelli, J. W. Ochterski, P. Y. Ayala, K. Morokuma, G. A. Voth, P. Salvador, J. J. Dannenberg, V. G. Zakrzewski, S. Dapprich, A. D. Daniels, M. C. Strain, O. Farkas, D. K. Malick, A. D. Rabuck, K. Raghavachari, J. B. Foresman, J. V. Ortiz, Q. Cui, A. G. Baboul, S. Clifford, J. Cioslowski, B. B. Stefanov, G. Liu, A. Liashenko, P. Piskorz, I. Komaromi, R. L. Martin, D. J. Fox, T. Keith, M. A. Al-Laham, C. Y. Peng, A. Nanayakkara, M. Hallacomb, P. M. W. Gill, B. Johnson, W. Chen, M. W. Wong, C. Gonzalez and J. A. Pople, *GAUSSIAN 03, (Revision E.01)*, Gaussian, Inc., Wallingford, CT, 2004.